Korean J. Chem. Eng., **29**(10), 1438-1443 (2012)
DOI: 10.1007/s11814-012-0050-z

Computational study on the decomposition of tetraneopentyl zirconium for the chemical vapor deposition of zirconium carbide

Yong Sun Won†

Department of Chemical Engineering, Pukyong National University, Busan 608-739, Korea
(*Received 8 March 2012 • accepted 13 April 2012*)

Abstract−The overall gas phase decomposition mechanism of tetraenopentyl zirconium precursor ($Zr[CH_2C(CH_3)_3]_4$) for the chemical vapor deposition of zirconium carbide thin films was investigated by using computational thermochemistry. Density functional theory (DFT) and harmonic vibrational frequency calculation were used to generate thermodynamic properties at each reaction step, based on which thermodynamic or kinetic preference of a reaction pathway was evaluated. While the preference of γ-hydrogen abstraction of neopentane over α-hydrogen abstraction was confirmed in the initial stage of $ZrNp_4$ decomposition, they turned out to be competing instead of the dominant preference of γ-hydrogen abstraction. Methane formation at three subsequent reaction steps was explained by β-methyl migration, and the following α-hydrogen abstraction of methane based on the suggestion that α- and γ-hydrogen abstractions of neopentane are competing kinetically in previous reaction steps. Computational thermochemistry showed a possibility as a general tool to anticipate the gas phase decomposition mechanism of a precursor in chemical vapor deposition.

Key words: Tetraneopentyl Zirconium, Zirconium Carbide, Chemical Vapor Deposition, Density Functional Theory

INTRODUCTION

Zirconium carbide (ZrC) is one of the promising cathode materials in the application of FEAs (field emitter arrays), featuring its great hardness (25,467 N/mm^2), high melting point (3,400 °C), high electrical conductivity (50×10^{-6} Ω-cm) and low work function (4.0 eV) compared to the conventionally used silicon (4.52 eV) and molybdenum (4.6 eV) [1-3]. Fabrication of cathodes from low work function and hard materials like ZrC or coating of those materials on conventional cathodes, such as silicon and molybdenum, is expected to increase the current density without cathode failure (vacuum arc or tip dulling): high brightness electron source with longevity is achieved [4-9].

Metal-organic chemical vapor deposition (MOCVD) is widely used for the high quality thin film growth with its advantages in low temperature film formation and uniform coverage of small features. Several successful MOCVD growths of ZrC thin films using the single source metalorganic tetraneopentyl zirconium ($Zr[CH_2C(CH_3)_3]_4$, alias $ZrNp_4$) have been reported in the temperature range 300 to 800 °C. The films, however, were not stoichiometric, but contained excess carbon in an approximate Zr/C ratio of 1 : 2 to 5. Moreover, they were performed only at relatively low pressure (<10^{-4} Torr) because $ZrNp_4$ is less-volatile [10-13]. Recently, we have reported the amorphous ZrC thin film growth by aerosol-assisted MOCVD using $ZrNp_4$ at half an atmospheric pressure and in the temperature range 400 to 600 °C, where the limit of less-volatility was lifted via the so-called nebulization step to convert the precursor solution ($ZrNp_4$+ benzonitrile solvent) into aerosols, which are sprayed and heated on the substrates [14,15].

The decomposition mechanism of $ZrNp_4$ in the gas phase under the CVD conditions is very important to understand the deposition behavior directly or indirectly. Although several theoretical and experimental researches about the initial decomposition mechanism of $ZrNp_4$ confirmed the preference of γ-hydrogen abstraction over α-hydrogen abstraction [16-18], the overall mechanism has not been proposed yet. In addition, the observation of significant amounts of methane in the $ZrNp_4$ decomposition [13] was not explained. In this study, we propose possible gas phase decomposition pathways of $ZrNp_4$, based on the computational thermochemistry. This approach can be generally applied to anticipate the gas phase decomposition mechanism of an unknown (or novel) precursor.

COMPUTATIONAL METHOD

All calculations were carried out with the GAUSSIAN 03 programs [19], along with B3LYP DFT (density functional theory) method and split basis set (LanL2DZ for zirconium and 6-31G(d) for other elements) [20,21]. Full geometry optimization was carried out for all species. The transition state (TS) was optimized using the Berny alogrithm as implemented in the GAUSSIAN 03 program. Harmonic vibration frequencies were calculated for each structure, based on which thermodynamic properties such as enthalpy and Gibbs free energy were computed for thermochemistry analysis. The GaussView program was used for the visualization of the results.

RESULTS AND DISCUSSION

1. Initial Stage of the Decomposition of $ZrNp_4$

Experimental and theoretical studies on the thermolysis of tetraneopentyltitanium ($TiNp_4$) proposed two possible reactions - α-hydrogen abstraction and γ-hydrogen abstraction - as the initial step in the decomposition of $TiNp_4$, and the preference is for α-hydrogen abstraction over γ-hydrogen abstraction [16-18].

†To whom correspondence should be addressed.
E-mail: yswon@pknu.ac.kr

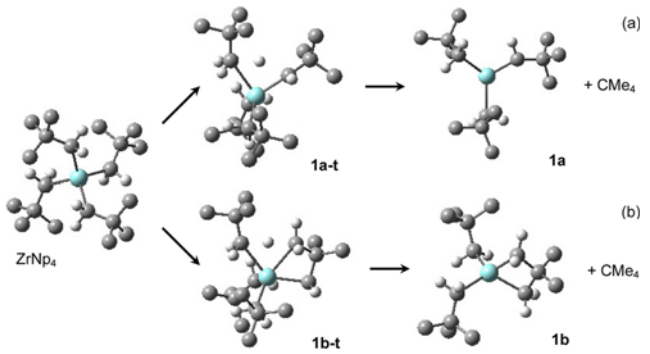

Fig. 1. Initial decomposition steps for $ZrNp_4$; (a) α-hydrogen abstraction and (b) γ-hydrogen abstraction.

$$TiNp_4 \xrightarrow{\alpha\text{-hydrogen abstraction}} Np_2Ti{=}\langle^{H}_{(t\text{-Bu})} + CMe_4\ (Neopentane) \quad (1)$$

$$TiNp_4 \xrightarrow{\gamma\text{-hydrogen abstraction}} Np_2Ti\langle\rangle + CMe_4 \quad (2)$$

By analogy, the same initial decomposition reactions are constructed for $ZrNp_4$ as shown in Fig. 1. Geometries of transition complexes (**1a-t**, **1b-t**) and products (**1a**, **1b**) were consistent with ones obtained by Wu et al. using molecular orbital theory (HF/3-21G) [16] instead of DFT used in this study. To determine the preference, the energetics of those two pathways and the homolysis of neopentyl (for comparison) in the initial step of $ZrNp_4$ decomposition were listed and compared in Table 1. Apparently, decomposition pathways such as α-hydrogen abstraction (entry 1) and γ-hydrogen abstraction (entry 2) are much more favorable in energetics (by about more than 25 kcal/mol) than the homolysis of neopentyl (entry 5). For comparison, the $\Delta H^{o,\ddagger}_{298}$ of the homolysis of benzyl from tetrabenzyl zirconium ($ZrBn_4$) is 45.6 kcal/mol, which has a small difference of about 5 kcal/mol in activation energy from α- or γ-hydrogen abstraction from $ZrNp_4$ (entry 1 or 2). It indicates the homolysis of benzyl from $ZrBn_4$ readily occurs in the typical temperature range of MOCVD, 400 to 800 °C. Moreover, it explains the reason why there have been no reports on ZrC film growth using $ZrBn_4$ so far and our trials of ZrC film growth using $ZrBn_4$ also failed [14].

In terms of equilibrium thermodynamics, α- and γ-hydrogen abstractions (entry 3 and 4) are both endothermic and γ-hydrogen abstraction is more spontaneous because its product (**1b**) still maintains the original stable tetrahedral configuration between zirconium and four nearest carbons by forming a ring at one side. Also in terms of kinetics, γ-hydrogen abstraction is more favorable, having lower activation energy. It is consistent with the theoretical and experimental results reported by Wu et al. [16]. The calculated difference in $\Delta G^{o,\ddagger}_{298}$ values between two hydrogen abstractions from $ZrNp_4$ is only about 1.7 kcal/mol, corresponding to 17 times faster γ-hydrogen abstraction over α-hydrogen abstraction at 298 K or 3.0 to 3.5 times faster at 400 to 500 °C, according to TST (transition state theroy) kinetics. For comparison, Wu et al. determined γ-hydrogen abstraction is 4.9 times faster at the same temperature range (400 to 500 °C), through an experimental study using MS (mass spectroscopy) and deuterium labeled $ZrNp_4$ [16]. Therefore, one of the two pathways is not overwhelming to the other but instead they are competing, even if γ-hydrogen abstraction is a little more favorable. Wu et al. also reported computational analysis results using molecular orbital theory to support their experimental study [16]. However, the difference of $\Delta G^{o,\ddagger}_{298}$ values of α- and γ-hydrogen abstractions using HF/3-21G was 5.9 kcal/mol in their calculation. Although an adjustment on the basis of comparison with the results obtained for $ZrMe_4$ using HF/6-31G and MP2/HW3 lowered the difference of $\Delta E^{\ddagger}$ values of α-and γ-hydrogen abstractions by 1.4 kcal/mol [16], their calculation still expected the dominant preference of γ-hydrogen abstraction compared to ours by three orders of magnitude (~2,000 times faster) at 298 K. The calculation using HF method with the same basis set in our calculation also generated a big difference of $\Delta G^{o,\ddagger}_{298}$ values (3.1 kcal/mol), corresponding to the preference of γ-hydrogen abstraction by two orders of magnitude (~180 times faster), as shown in Table 1 (entry 6 and 7).

The activation energy of γ-hydrogen abstraction of $ZrNp_4$ is worthwhile to be compared to the activation energy of α-hydrogen abstraction of $TiNp_4$. It was confirmed theoretically and experimentally that α-hydrogen abstraction is more favorable in the initial decomposition of $TiNp_4$ due to its larger release of steric interactions [17,18]. The activation energy of the α-hydrogen abstraction of $TiNp_4$, experimentally determined in solution, was 21.5±1.4 kcal/mol [18], and it is much lower compared to 37.4 kcal/mol, theoretically determined for the γ-hydrogen abstraction of $ZrNp_4$, as shown in Table 1. This big difference, even with the practical limit of theoretical calculation, is consistent with the reported MOCVD growth of TiC using $TiNp_4$ at temperatures as low as 150 °C, while 400 °C is the minimum deposition temperature in our AA-MOCVD of ZrC thin films using $ZrNp_4$ [14,15].

As a summary, γ-hydrogen abstraction in the initial decomposition of $ZrNp_4$ is preferred over α-hydrogen abstraction, but they are rather competing in the typical MOCVD conditions (400 to 800 °C) instead of the dominant preference of γ-hydrogen abstraction.

2. Overall Decomposition of $ZrNp_4$

For the further detailed study of the $ZrNp_4$ decomposition mech-

Table 1. Energetics of possible pathways for the initial $ZrNp_4$ decomposition

Entry	Reactions	ΔH^{o}_{298} or $\Delta H^{o,\ddagger}_{298}$ (kcal/mol)	ΔG^{o}_{298} or $\Delta G^{o,\ddagger}_{298}$ (kcal/mol)	Note
1	$ZrNp_4 \rightarrow$ **1a-t**	40.6‡	41.9‡	α-H abs., DFT
2	$ZrNp_4 \rightarrow$ **1b-t**	37.4‡	40.2‡	γ-H abs., DFT
3	$ZrNp_4 \rightarrow$ **1a**+CMe_4	30.1	18.0	DFT
4	$ZrNp_4 \rightarrow$ **1b**+CMe_4	3.1	−7.9	DFT
5	$ZrNp_4 \rightarrow Np_3Zr\bullet + \bullet Np$	57.1	42.6	Homolysis, DFT
6	$ZrNp_4 \rightarrow$ **1a-t**	60.3‡	61.6‡	α-H abs., HF
7	$ZrNp_4 \rightarrow$ **1b-t**	55.5‡	58.5‡	γ-H abs., HF

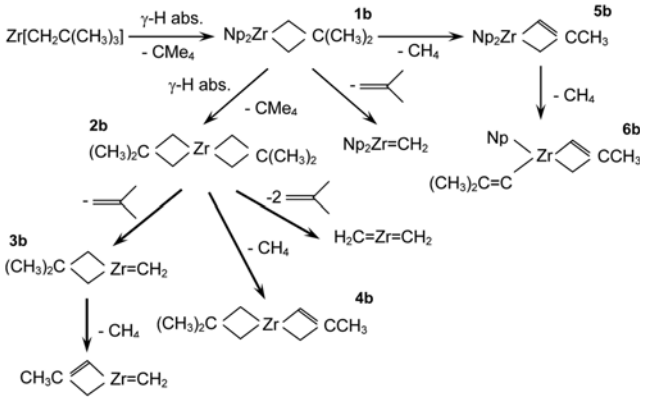

Fig. 2. Tentative decomposition pathways of $ZrNp_4$.

anism, a tentative decomposition mechanism of $ZrNp_4$ is constructed in Fig. 2, based on the information of the preference of γ-hydrogen abstraction discussed in the previous section. The following three pathways are major ones. The isobutene formation via a ring opening in the pathway (3) was suggested by Wu et al. [16]. However, pathways (4), (5), and the involved cleavage to CH_4 have not been reported.

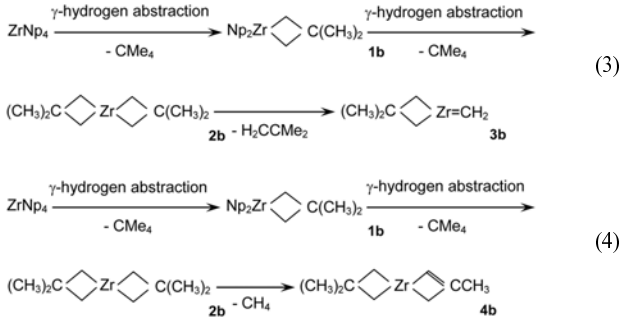

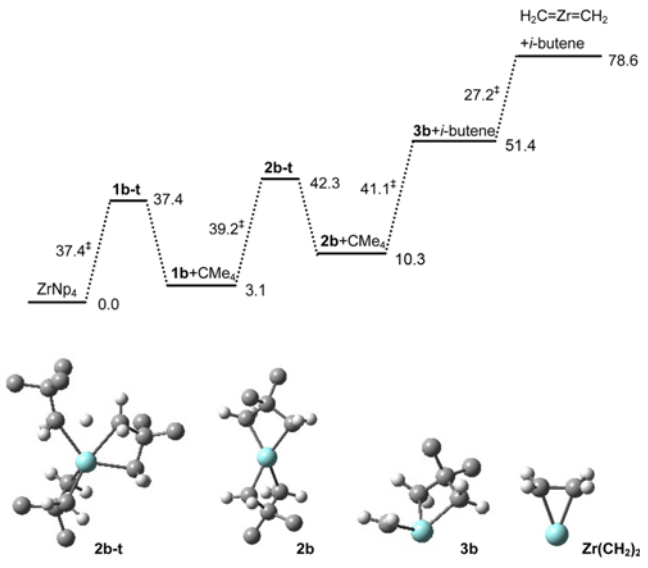

Fig. 3. Energetics of the reaction scheme (3) and computed structures of 2b-t (a transition state for the second γ-hydrogen abstraction), 2b, and 3b. All values in energetics are in the unit of kcal/mol.

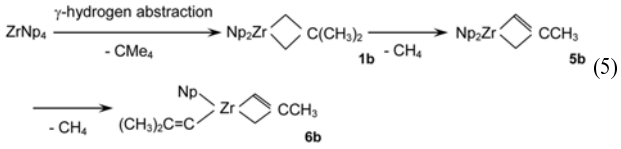

2-1. Reaction Scheme (3)

Fig. 3 shows the structures of **2b-t** (transition state for the second γ-hydrogen abstraction), **2b**, and **3b**. The tetrahedral structure between zirconium and four nearest carbons is still maintained in **2b** and explains the spontaneity (ΔG^{o}_{298}=−2.9 kcal/mol) of the reaction, **1b**→**2b**+CMe_4. For the formation of isobutene via a ring opening, the effort to locate the corresponding transition complex failed, but it is expected that the transition structure is close to the reaction product [16]. Accordingly, the structure of **3b** shows an empty coordination site which likely isobutene used to occupy. The activation energy of **1b**→**2b** and ΔH^{o}_{298} of **2b**→**3b**, as shown in Fig. 3, indicate these reactions are accessible in the typical MOCVD growth temperature range, 400 to 800 °C. The structure of **3b**, tetrahedral with an empty coordination site, proposes the participation of this molecule into the adsorption on the surface and the following heterogeneous deposition process using its empty coordination site. The second isobutene formation via the other ring opening from **3b** to form H_2C=Zr=CH_2 demands a smaller energy (ΔH^{o}_{298}=27.2 kcal/mol) compared to the first isobutene formation (**2b**→**3b**) due to the stable triangular structure of H_2C=Zr=CH_2, as shown in Fig. 3. Thus, **3b** or H_2C=Zr=CH_2 might be the last product in the reaction scheme (3) when the reaction occurs in the gas phase in the typical growth temperature range of MOCVD.

2-2. Reaction Scheme (4) & (5)

Healy et al. reported the evidence for significant quantities of methane in the $ZrNp_4$ decomposition, along with neopentane and isobutene [13]. Reaction schemes (4) and (5) have several pathways for CH_4 formation via a reductive elimination, but they are just proposed ones to be verified by computational thermochemistry as done so far. Fig. 4 shows a possible transition state for the first CH_4 formation (**5b-t**), and the structure of **5b**. The energetics

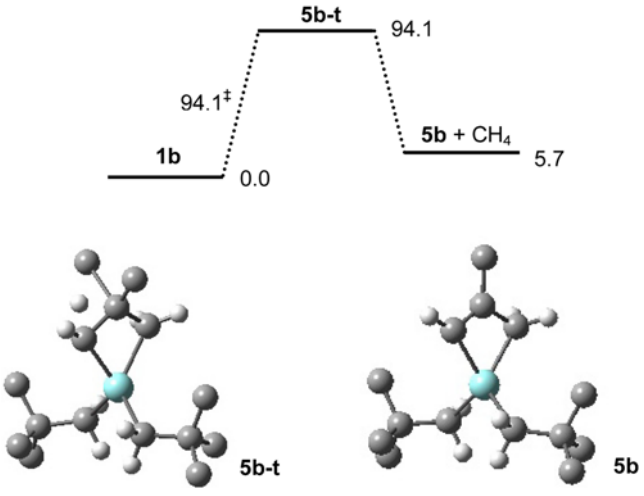

Fig. 4. Energetics of the first CH_4 formation from 1b to 5b and computed structures of 5b-t (a transition state for the first CH_4 formation) and 5b. All values in energetics are in the unit of kcal/mol.

for this reaction is also summarized in Fig. 4. Because of the effect of entropy increase (1 mol→2 mol) and the still stable tetrahedral structure between zirconium and four nearest carbons in **5b**, ΔG^{o}_{298} of the reaction is negative (−6.24 kcal/mol), thermodynamically accessible. However, the high activation energy barrier of **5b-t** ($\Delta H^{o,\ddagger}_{298}$ =94.1 kcal/mol) suggests this pathway is not viable in the gas phase in the conventional MOCVD conditions.

Because reaction scheme (5) has two successive CH_4 formations and **1b** has two neopentyl ligands, direct CH_4 formation from a neopentyl ligand ($CH_2CMe_3 \rightarrow CHCMe_2+CH_4$) was checked. It also turned out to have a high activation energy ($\Delta H^{o,\ddagger}_{298}$=91.4 kcal/mol) but slight overall exothermicity (ΔH^{o}_{298}=7.8 kcal/mol), similar to the previously calculated pathway for CH_4 formation. Thus, a different explanation is needed for the CH_4 formation in reaction scheme (4) and (5).

2-3. Methane Cleavage

The β-methyl migration and subsequent CH_4 cleavage provide another probable mechanism for this. The β-methyl elimination from cationic neopentyl complexes has been demonstrated to be a facile step in eliminating isobutene [22-25]. A kinetic study of the β-methyl elimination in $B(C_6F_5)_3$-derived Zr metallocenium ion-pairs showed the activation energy ($\Delta H^{o,\ddagger}$) was 22.5 (0.9) kcal/mol for the β-methyl elimination as shown in the following reaction [26].

$$[(1,2\text{-}Me_2Cp)_2ZrCH_2(t\text{-}Bu)]^+[CH_3B(C_6F_5)_3]^- \xrightarrow{\beta\text{-methyl elimination}} [(1,2\text{-}Me_2Cp)_2ZrCH_3]^+[CH_3B(C_6F_5)_3]^- + \text{isobutene}$$

The reactant complex contains both Zr and neopentyl ligand. Thus, β-methyl migration is assumed to be possible in the $ZrNp_4$ decomposition. However, the location of the corresponding transition state is technically challenging. Therefore, only the identification of the intermediate resulting from β-methyl migration and the following CH_4 cleavage will be demonstrated with the assumption that β-methyl migration is a fast step as suggested in the literature [22-26].

In reaction scheme (4), CH_4 formation follows successive γ-hydrogen abstractions, but the intermediate **2b** does not seem to have a favorable geometry to donate a methyl to zirconium because tetrahedral structure is already maintained between zirconium and four nearest carbons in **2b**. Thus, another intermediate is chosen to explain CH_4 formation, which is the product of one α-hydrogen abstraction and one γ-hydrogen abstraction, because α-hydrogen abstraction competes with γ-hydrogen abstraction to a certain extent, as previously suggested. Fig. 5 shows the geometry of this intermediate (**2b′**). It has an empty coordination site to which a methyl could migrate. A possible intermediate via β-methyl migration, a transition state for the following CH_4 cleavage, and the resulting final product (**4b′**) are shown in Fig. 5. The energetics for this reaction is also summarized in Fig. 5.

Fig. 5 demonstrates β-methyl migration is highly exothermic. The interatomic distance of Zr-C1 bond is increased from 1.980 Å to 2.223 Å and the one of C1-C2 bond is decreased from 1.514 Å to 1.354 Å, as a result of β-methyl migration. It suggests the following bond order changes: for Zr-C1, double→single, for C1-C2, single →double. Then, the following CH_4 cleavage has an accessible activation energy (35.9 kcal/mol), and it is also thermodynamically favorable. The ΔG^{o}_{298} for CH_4 cleavage is 4.2 kcal/mol, but it will become negative as the temperature increases because of its positive ΔS^{o} (1 mol→2 mol). Although the transition state corresponding to β-methyl migration has not yet been located, the energetics of the sub-

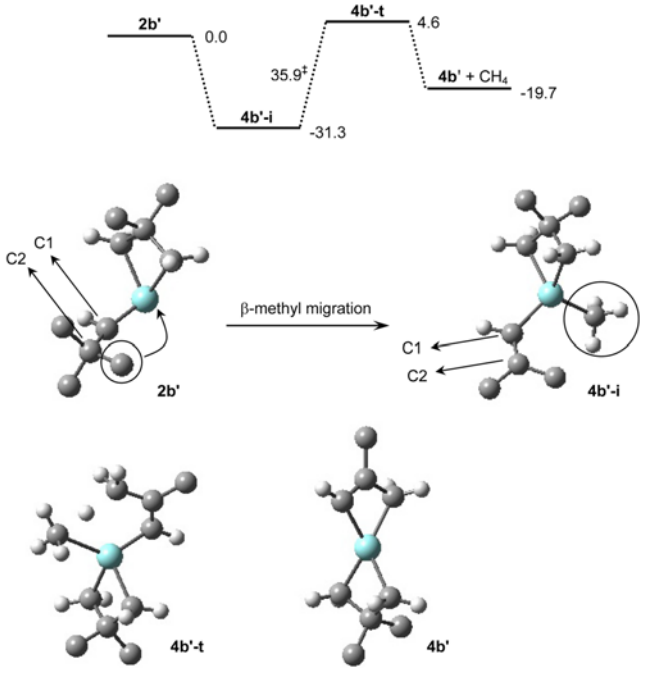

Fig. 5. Energetics of β-methyl migration from 2b′ and subsequent CH_4 cleavage, and computed structures of 2b′, 4b′-i (an intermediate via β-methyl migration), 4b′-t (a transition state for the following CH_4 cleavage), and 4b′. All values in energetics are in the unit of kcal/mol.

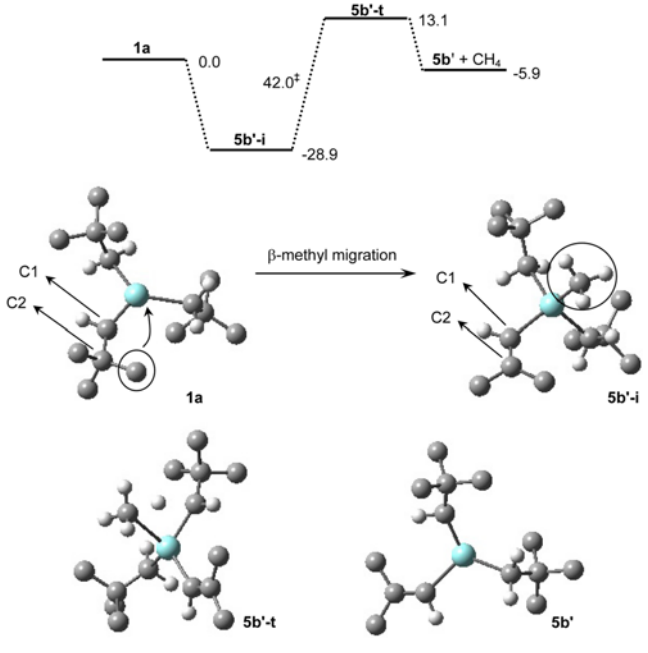

Fig. 6. Energetics of β-methyl migration from 1a and the subsequent CH_4 cleavage, and computed structures of 1a, 5b′-i (an intermediate via β-methyl migration), 5b′-t (a transition state for the following CH_4 cleavage), and 5b′. All values in energetics are in the unit of kcal/mol.

sequent reactions suggests the proposed scheme involving the β-methyl migration could be a possible explanation for CH_4 formation.

Formation of CH_4 via the reaction scheme (5) has also been investigated by the same approach including β-methyl migration. Again, because the γ-hydrogen abstraction product, **1b**, does not have a proper geometry for the methyl shift, the α-hydrogen abstraction product, alkylidene **1a** (see Fig. 1), was chosen as a starting point instead. Fig. 6 shows the geometry of **1a** and a possible intermediate (**5b′-i**) from β-methyl migration and energetics of this reaction. Migration of the β-methyl to Zr is highly exothermic as demonstrated in Fig. 6. The Zr-C1 bond is increased from 2.008 Å to 2.219 Å and C1-C2 is decreased from 1.518 Å to 1.354 Å, as a result of β-methyl migration. It suggests the following bond order changes: for Zr-C1, double→single, for C1-C2, single→double. The following CH_4 cleavage occurs via α-hydrogen abstraction from a neopentyl ligand to leave behind -$CHCMe_3$, which is the methyl source for the next CH_4 formation via β-methyl migration. The reaction also has a viable activation energy as shown in Fig. 6 but CH_4 cleavage via α-hydrogen elimination itself has unfavorable energetics (ΔG^{o}_{298}= 25.8 kcal/mol) compared to the previous case (ΔG^{o}_{298}= 4.2 kcal/mol). The ring formation (**4b'-t** and **4b'** in Fig. 5) in the previous case is attributed to its favorable energetics. However, the overall reaction (ΔG^{o}_{298}=−5.9 kcal/mol) is still thermodynamically favorable due to its stabilized intermediate, **5b'-i**, and entropy effect (positive ΔS^{o}). As mentioned, the second CH_4 formation will be initiated with β-methyl migration from the newly formed -$CHCMe_3$ ligand.

The activation energies for the main steps - α-hydrogen abstraction (40.6 kcal/mol in Table 1), γ-hydrogen abstraction (37.4 kcal/mol in Table 1 and 39.2 kcal/mol in Fig. 3), isobutene cleavage (41.1 kcal/mol in Fig. 3) and CH_4 formation via β methyl migration (35.9 kcal/mol in Fig. 5 and 42.0 kcal/mol in Fig. 6) - are all in the narrow range, 37 to 42 kcal/mol. These results suggest that these reactions should be competitive in the temperature range used for MOCVD. Fig. 7 illustrates the postulated decomposition mechanism of $ZrNp_4$ in the gas phase under the conventional MOCVD conditions (400 to 800 °C), based on the results obtained from computational chemistry. Reaction steps having too high activation barriers such as CH_4 formation from $C_6H_{12}Zr$ to form C_5H_8Zr, as previously presented, are omitted in Fig. 7.

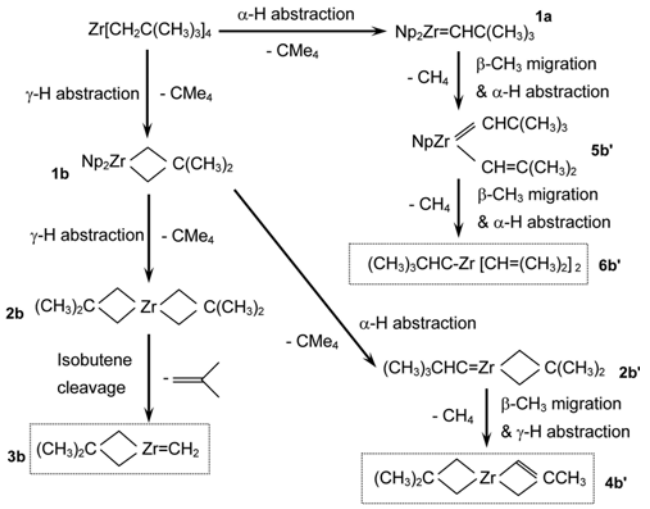

Fig. 7. Decomposition pathways of $ZrNp_4$ in the gas phase under the conventional MOCVD conditions (400 to 800 °C), based on the computational results.

The decomposition of $ZrNp_4$ in the gas phase stops at one of these intermediates, **3b**, **4b′**, or **6b′**. They are all saturated because no simple dissociation is involved and three (**3b** and **6b′**) or four (**4b′**) carbons surround zirconium. Thus, if they participate in heterogeneous reactions for film growth, C/Zr ratio in the deposited film will likely be greater than stoichiometric value of ZrC without considering H_2 reducing effect. As an illustration, **3b** has an empty coordination site that is potentially usable for the adsorption on the surface. Then, isobutene will be possibly cleaved off from the ring side to leave behind $H_2C{=}Zr{=}CH_2$ (ad). It has two strong double bonds probably to result in C/Zr~2 in the deposited film. However, **3b** will be the main starting complex for the subsequent heterogeneous reactions because of its adsorption-favorable structure. Its dipole moment was calculated as 3.12 Debye and it was 0.66 Debye for **4b′** for comparison. Further study is required for the details of the heterogeneous reaction mechanism for film growth.

CONCLUSION

In the initial stage of $ZrNp_4$ decomposition, the preference of γ-hydrogen abstraction over α-hydrogen abstraction was confirmed, but they were rather competing instead of the dominant preference of γ-hydrogen abstraction. The overall decomposition mechanism of $ZrNp_4$ was proposed and verified by computational thermochemistry. The mechanism of the reported significant quantities of methane in the $ZrNp_4$ decomposition was explained reasonably by β-methyl migration and the subsequent α-hydrogen abstraction of methane at individual reaction steps. The fact that α- and γ-hydrogen abstractions are competing plays an important role in the interpretation of methane formation steps. The gas phase decomposition of $ZrNp_4$ turned out to end at still sizable intermediates containing at least three nearest carbons to zirconium, so that C/Zr ratio higher than its stoichiometric value (1 : 1) in the deposited film in several MOCVD growth reports using $ZrNp_4$ seems to be explanative. As a summary, computational thermochemistry would be very useful to anticipate the gas phase decomposition of an unknown (or novel) precursor in the CVD growth preliminarily.

ACKNOWLEDGEMENTS

This research was a part of the project titled “Development of key technology in seawater desalination using gas hydrate process” funded by the Ministry of Land, Transport and Maritime Affairs, Korea. All the calculation works were done in the author’s graduate study and thus the author appreciates the Department of Chemistry at University of Florida granting the access to the Gaussian software.

REFERENCES

1. R. Kieffer, *Proc. Intern. Symp. Reactive Solids*, 1001 (1952).
2. Technical Publications, CERAO Incorporate, **7**(2) (1997).
3. T. Aizawa, *T. Rep. National Inst. Res. Inorg. Mater.*, **81**, 27 (1994).
4. W. A. Mackie, R. L. Hartman, M. A. Anderson and P. R. Davis, *J. Vac. Sci. Technol. B*, **12**(2), 722 (1994).

5. W. A. Mackie, T. Xie, M. R. Matthews, B. P. Routh Jr. and P. R. Davis, *J. Vac. Sci. Technol. B*, **16**(4), 2057 (1998).
6. W. A. Mackie, T. Xie and P. R. Davis, *J. Vac. Sci. Technol. B*, **17**(2), 613 (1999).
7. D. H. Kang, V. V. Zhirnov, G. J. Wojak, R. C. Sanwald, M. Park, J. J. Hren and J. J. Cuomo, *Mat. Res. Soc. Symp. Proc.*, **558**, 563 (2000).
8. C. Spindt, C. E. Holland and P. R. Schwoebel, *SPIE Proc.*, **3955**, 151 (2000).
9. J. E. Yater, A. Shih and D. S. Katzer, *Mat. Res. Soc. Symp. Proc.*, **558**, 551 (2000).
10. D. C. Smith, R. R. Rubiano, M. D. Healy and R. W. Springer, *Mat. Res. Soc. Symp. Proc.*, **282**, 642 (1993).
11. J. E. Parmeter, D. C. Smith and M. D. Healy, *J. Vac. Sci. Technol. A*, **12**(4), 2107 (1994).
12. G. S. Girolami, J. A. Jensen, J. E. Gozum and D. M. Pollina, *Mat. Res. Soc. Symp. Proc.*, **121**, 429 (1998).
13. M. D. Healy, D. C. Smith, R. R. Rubiano, R. W. Springer and J. E. Parmeter, *Mat. Res. Soc. Symp. Proc.*, **327**, 127 (1994).
14. Y. S. Won, Y. S. Kim, O. Kryliouk, T. J. Anderson, V. G. Varanasi, C. T. Sirimanne and L. McElwee-White, *J. Cryst. Growth*, **304**, 324 (2007).
15. Y. S. Won, V. G. Varanasi, O. Kryliouk, T. J. Anderson, L. McElwee-White and R. J. Perez, *J. Cryst. Growth*, **307**, 302 (2007).
16. Y. D. Wu, Z. H. Peng, K. W. K. Chan, L. Xiaozhan, A. A. Tuinman and Z. Xue, *Organometallics*, **18**, 2081 (1999).
17. Y. D. Wu, Z. H. Peng and Z. Xue, *J. Am. Chem. Soc.*, **118**, 9772 (1996).
18. J. W. Cheon, H. D. Lawrence and G. S. Girolami, *J. Am. Chem. Soc.*, **119**, 6814 (1997).
19. Gaussian 03, Revision B.04, M. J. Frisch, G. W. Trucks, H. B. Schlegel, G. E. Scuseria, M. A. Rob, J. R. Cheeseman, J. A. Montgomery Jr., T. Vreven, K. N. Kudin, J. C. Burant, J. M. Millam, S. S. Iyengar, J. Tomasi, V. Barone, B. Mennucci, M. Cossi, G. Scalmani, N. Rega, G. A. Petersson, H. Nakatsuji, M. Hada, M. Ehara, K. Toyota, R. Fukuda, J. Hasegawa, M. Ishida, T. Nakajima, Y. Honda, O. Kitao, H. Nakai, M. Klene, X. Li, J. E. Knox, H. P. Hratchian, J. B. Cross, V. Bakken, C. Adamo, J. Jaramillo, R. Gomperts, R. E. Stratmann, O. Yazyev, A. J. Austin, R. Cammi, C. Pomelli, J. W. Ochterski, P. Y. Ayala, K. Morokuma, G. A. Voth, P. Salvador, J. J. Dannenberg, V. G. Zakrzewski, S. Dapprich, A. D. Daniels, M. C. Strain, O. Farkas, D. K. Malick, A. D. Rabuck, K. Raghavachari, J. B. Foresman, J. V. Ortiz, Q. Cui, A. G. Baboul, S. Clifford, J. Cioslowski, B. B. Stefanov, G. Liu, A. Liashenko, P. Piskorz, I. Komaromi, R. L. Martin, D. J. Fox, T. Keith, M. A. Al-Laham, C. Y. Peng, A. Nanayakkara, M. Challacombe, P. M. W. Gill, B. Johnson, W. Chen, M. W. Wong, C. Gonzalez and J. A. Pople, Gaussian, Inc., Wallingford CT, 2004.
20. A. D. Becke, *J. Chem. Phys.*, **98**, 1372 (1993).
21. P. J. Stephens, F. J. Devlin, C. F. Chabalowski and M. J. Frisch, *J. Phys. Chem.*, **98**, 11623 (1994).
22. S. Hajela and J. E. Bercaw, *Organometallics*, **13**, 1147 (1994).
23. A. D. Horton, *Organometallics*, **15**, 2675 (1996).
24. M. Lin, G. J. Spivak and M. C. Baird, *Organometallics*, **21**, 2350 (2002).
25. P. J. Chirik, N. F. Dalleska, L. M. Henling and J. E. Bercaw, *Organometallics*, **24**, 2789 (2005).
26. C. L. Beswick and T. J. Marks, *J. Am. Chem. Soc.*, **122**, 10358 (2000).